PHYSICAL REVIEW B **95**, 140403(R) (2017)

Incommensurate magnetic order in a quasicubic structure of the double-perovskite compound Sr_2NiIrO_6

K. Rolfs,[1,*] S. Tóth,[2,3] E. Pomjakushina,[1] D. T. Adroja,[4,5] D. Khalyavin,[4] and K. Conder[1]

[1]*Laboratory for Scientific Developments and Novel Materials, Paul Scherrer Institut, CH-5232 Villigen, Switzerland*

[2]*Laboratory for Neutron Scattering and Imaging, Paul Scherrer Institut, CH-5232 Villigen, Switzerland*

[3]*Laboratory for Quantum Magnetism, ICMP, Ecole Polytechnique Federale de Lausanne (EPFL), CH-1015 Lausanne, Switzerland*

[4]*ISIS Pulsed Neutron and Muon Source, STFC Rutherford Appleton Laboratory, Harwell Campus, Didcot, Oxfordshire, OX11 0QX, United Kingdom*

[5]*Highly Correlated Matter Research Group, Physics Department, University of Johannesburg, P.O. Box 524, Auckland Park 2006, South Africa*

(Received 26 October 2016; revised manuscript received 16 March 2017; published 10 April 2017)

In Sr_2NiIrO_6, a metastable compound, the magnetic structure could be elucidated. The magnetic susceptibility data of the compound suggests a three-dimensional Heisenberg behavior. Moreover, neutron diffraction reveals a novel incommensurate magnetic order, requiring exchange interactions beyond second neighbor to stabilize this phase. An incommensurate propagation vector of $\mathbf{k} = (0,k,k)$ with $k = 0.356$ was observed in such a pseudocubic system. This can be an example of how to induce an incommensurate ground state and a possible type-II multiferroicity in double perovskites.

DOI: 10.1103/PhysRevB.95.140403

In the field of strongly correlated electron systems significant attention has been drawn toward the study of compounds based on magnetic *4d* and *5d* transition-metal (TM) oxides. The spin-orbit coupling (SOC) within these systems becomes non-negligible compared to the crystal-field energies. This can lead to new exotic phases, such as the Mott insulating state of Sr_2IrO_4 [1] and Na_2IrO_3 [2]. Motivated by these findings, new models that include the strong SOC have been developed and several new ground states were predicted [3]. However, often the experimental results and theoretical models deviate significantly as reported for the magnetic honeycomb materials A_2IrO_3 with A = Na,Li [4–6]. In order to understand the influence of the SOC on the electronic ground state the focus also turned to mixed 3*d*-5*d* systems. In these systems, it might be possible to disentangle the SOC from other effects, such as common charge-spin-orbital physics. This results in a more precise understanding of how strong SOC changes the electronic ground state. Moreover, these materials can have magnetic ground states that are interesting in their own right.

The family of double perovskites is known for a potpourri of compelling properties, such as multiferroicity in Bi_2NiReO_6 or Bi_2MnReO_6 [7], the giant magnetoresistance found in Mn_2FeReO_6 [8], as well as uncommon magnetic ground states, such as the spin-glass state found in Sr_2YReO_6 [9]. One interesting group within these hybrid oxides is the group of Ir-based double perovskites with formula A_2MIrO_6 ($M = 3d$ TM). Most of the Sr_2MIrO_6 compounds are metastable and require high-pressure synthesis. One member, Sr_2NiIrO_6, has been successfully synthesized by Kayser *et al.* [10]. It was reported that Sr_2NiIrO_6 is a distorted tetragonal double perovskite at room temperature; crystal structure is shown in Fig. 1. Also, an antiferromagnetic phase transition was observed at 58 K; however, the magnetic structure was not determined. The compound has two structural phase transitions at 400 and 700 K changing from the low-temperature monoclinic structure ($P2_1/n$) to tetragonal ($I4/m$) and then to cubic ($Fm\bar{3}m$).

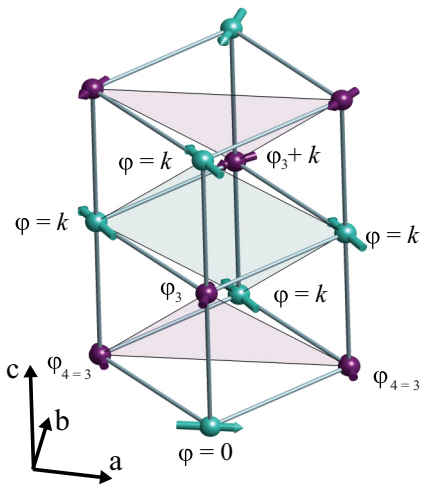

FIG. 1. Crystal and magnetic structures of Sr_2NiIrO_6 with green and purple spheres denoting nickel and iridium atoms, respectively. The semitransparent planes are normal to the measured magnetic propagation vector.

Based on density functional calculations, Ou *et al.* predicted a collinear magnetic ground state of Sr_2NiIrO_6 and competing ferromagnetic nickel-iridium and antiferromagnetic iridium-iridium interactions [11]. Since the nickel-iridium nearest-neighbor couplings are ferromagnetic, further neighbor interactions have to be taken into account to describe the observed antiferromagnetic transition. This is surprising, since the almost 180° Ni-O-Ir superexchange bonds are usually dominating for *3d* TM perovskites. These results suggest that the magnetism of Sr_2NiIrO_6 is strongly influenced by further neighbor exchanges [11].

Using the high oxygen pressure furnace [12], polycrystalline Sr_2NiIrO_6 was synthesized at 1173 K and 20 MPa

*katharina.rolfs@psi.ch

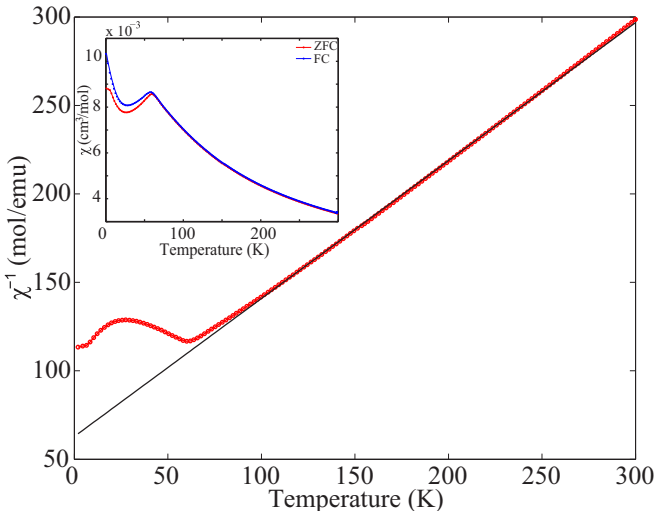

FIG. 2. The inverse magnetic susceptibility of Sr_2NiIrO_6 and the Curie-Weiss fit are shown as red and black lines, respectively. The inlet shows the field-cooled and zero-field-cooled susceptibility at 0.1 T magnetic field.

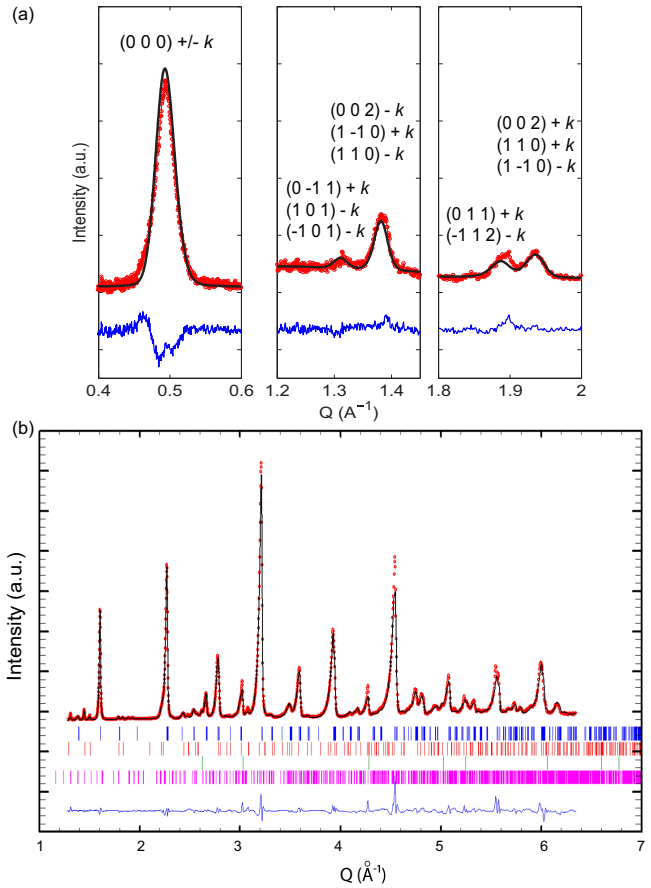

FIG. 3. (a) Difference between the 1.8 and 70 K diffraction data of Sr_2NiIrO_6 showing magnetic reflections only, denoted by red circles. Rietveld refinement and the deviation from the data is shown by black and blue lines, respectively. (b) Rietveld refinement of both the crystal and magnetic structures of Sr_2NiIrO_6.

of oxygen pressure. The precursor was synthesized with the citrate-nitrate method as described elsewhere [10]. The magnetic susceptibility of the compound was measured between 2.1 and 300 K using the Magnetic Property Measurement System (MPMS, Quantum Design). The low-temperature crystal and magnetic structure was determined by measuring a 2.5 g sample on the time-of-flight neutron diffractometer WISH at ISIS, UK. Diffraction patterns were collected between 1.8 and 70 K in 5 K steps.

Our Sr_2NiIrO_6 sample shows an antiferromagnetic phase transition at $T_N = 59$ K visible as a drop in the magnetic susceptibility upon cooling and deviating field-cooled (FC) and zero-field-cooled (ZFC) values at lower temperatures (see Fig. 2). Furthermore, the high-temperature behavior can be well described by the Curie-Weiss law. The model fit between 100 and 300 K gives a Curie-Weiss temperature of $T_{CW} = -81$ K, an effective moment of $3.20\mu_B$ averaged over nickel and iridium sites, and a Curie constant of 1.21 emu mol^{-1} K^{-1}. The $T_{CW}/T_N = 1.4$ factor suggests that magnetic frustration is present in Sr_2NiIrO_6. Although the observed Néel temperature agrees with previous report [10], we did not observe the nonlinear behavior of the inverse susceptibility above 100 K or a divergence of the FC and ZFC susceptibilities at high temperature. The previously reported anomalies were attributed to the temperature-dependent charge fluctuation between Ir^{+6}-Ni^{+2} and Ir^{+5}-Ni^{+3} states. Thus, our susceptibility data suggests we have a single iridium and nickel oxidation state in our sample. In this case, the observed effective moment is too small. The theoretical moment value for $S = 1$ Ni^{2+} and $J_{\text{eff}} = 3/2$ Ir^{+6} is $4.8\mu_B$ assuming gyromagnetic ratio $g = 2$ on both magnetic sites. However, as was shown before, the effective g factor can be notably reduced from the free-electron value in iridates [13,14] due to the hybridization with surrounding atomic oxygen or due to the noncubic point-group symmetry [15].

We also measured the neutron diffraction of Sr_2NiIrO_6 above and below the magnetic phase transition. We observed weak magnetic reflections appearing upon cooling at 60 K, revealing long-range magnetic order. In addition, no structural phase transition is visible below room temperature. The magnetic reflections can be separated by subtracting the 70 K data from the 1.8 K data [see Fig. 3(a)]. We could identify magnetic reflections at 0.49, 1.31, 1.40, 1.90, and 1.94 Å^{-1}, whereupon the first has the strongest intensity. All magnetic reflections can be indexed with the incommensurate propagation vector of $(0,k,k)$ with $k = 0.356$. This propagation vector suggests an accidental degeneracy of the ground state, since there are no lattice symmetry operations between the b and c axes in the monoclinic phase. We also determined the integrated intensity of the $(0,k,k)$ magnetic Bragg peak as a function of temperature (see Fig. 4). The fitted power-law function reveals a second-order phase transition with a β critical exponent of 0.39(2).

We refined the low-temperature diffraction pattern using the Rietveld method implemented in FULLPROF [16]. Two datasets were fitted simultaneously, measured on different banks of the diffractometer, with a different Q range and

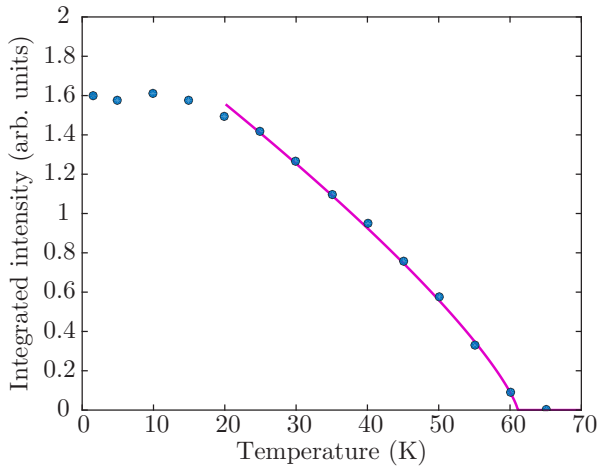

FIG. 4. Temperature dependence of the magnetic peak (000) $\pm k$ of Sr_2NiIrO_6 measured from 2 K up to 65 K, denoted by blue circles. Blue line denotes the best fit using a power-law function, best fit provides $T_N = 61.1(2)$ K, and critical exponent $\beta = 0.39(2)$.

resolution [17] [see Fig. 3(b)]. The fitted parameters of the monoclinic structural model are in good agreement with the previously reported values (see Table I for the atomic positions, site occupancies, and thermal displacement parameters). We also found a high level of ordering between the nickel and iridium sites, with 1:1 molar ratio between them. A small amount of impurities (less than 3 mol %) of $SrCO_3$ and NiO has been found, which does not influence the magnetic properties of the sample. Since the magnetic propagation vector is incommensurate, the most general magnetic structure is described by complex magnetization vectors and a relative phase φ on each of the four sublattices. Due to the large number of free parameters that describe the magnetic structure, the initial fit was achieved using a particle swarm optimization with randomly sampling coplanar elliptical structures. We could not improve the fit when noncoplanar structures were also included. Finally a further Rietveld refinement combining both the crystal and the magnetic structures achieved a reasonable agreement with the data [see Fig. 3(b)]. Some difference between the calculated and observed intensity is due to the strong neutron absorption of the sample. This varies over Q due to the geometry of the sample and instrument parameters, which we could not perfectly correct for. The goodness of the fit is given by an R_f factor of 2.63 and 4.65 for the structural parameters and $R_f = 7.53$ and 13.8 for the magnetic phase. Due to the weak magnetic signal compared to the measurement statistics, several magnetic structures gave similarly good fit. This includes sinusoidally modulated and helical magnetic structures depending on the relative length of the real and imaginary parts of the complex magnetization vector. However, the size of the ordered moment on each site and the relative phases were identical in each refined structure. These values are shown in Table I. The size of the ordered moment on the Ni site is close to the theoretical value of $2\mu_B$, however, the ordered moment of the Ir site is strongly reduced from the expected $3\mu_B$ value.

TABLE I. Crystal and magnetic structural parameters for Sr_2NiIrO_6 refined in the $P2_1/n$ space group at 1.8 K. The lattice parameters are $a = 5.539(7)$ Å, $b = 5.506(7)$ Å, $c = 7.798(10)$ Å, and $\beta = 90.096(14)^\circ$. M and φ denote the absolute value of the magnetic moment and its phase.

Crystal structure					
Atom	x	y	z	Occ.	B_{iso}
Sr	0.999(3)	−0.002(1)	0.221(1)	1.000(2)	0.043(81)
Ni	1/2	0	0	0.986(22)	1.02(32)
Ir	1/2	0	1/2	0.968(21)	0.54(39)
O1	0.714(4)	0.277(3)	0.013(3)	1.011(16)	1.53(39)
O2	0.242(4)	0.222(3)	0.997(4)	0.999(17)	1.730(43)
O3	0.050(2)	0.528(2)	0.248(5)	1.000(15)	2.10(41)
Magnetic structure					
Atom	x	y	z	ϕ (2π)	M (μ_B)
Ni	1/2	0	0	0	1.82(26)
	0	1/2	1/2	$0.35591 = k$	1.82(26)
Ir	1/2	0	1/2	φ	1.09(9)
	0	1/2	0	φ	1.09(9)

We successfully synthesized polycrystalline Sr_2NiIrO_6 under oxygen pressure. Our samples show no sign of charge fluctuation found previously [10]. Neutron diffraction showed that at low temperature Ni can be found in the Ni^{2+} state only with $S = 1$. This also requires that all iridiums are in the Ir^{6+} state. The lack of charge fluctuations at higher temperatures is evidenced by the magnetic susceptibility, where the temperature dependence of the magnetization in the paramagnetic phase can be well described by the Curie-Weiss law in a broad temperature range. This shows that the moment size and consequently the charge state of the magnetic ions is temperature independent. Moreover, our susceptibility and neutron diffraction data suggest that the magnetism of Sr_2NiIrO_6 is highly isotropic. This can be attributed to the fact that the three valence electrons of Ir^{6+} are on a half-filled t_{2g} orbital, thus effectively canceling out the orbital contribution to the magnetic moment. Also, the measured $\beta = 0.39(2)$ critical exponent corresponds to $3d$ Heisenberg behavior ($\beta = 0.36$) [18], suggesting that bond-directional exchanges are negligible in this compound.

Our refined crystal and magnetic structure shows that the magnetic atoms are little affected by the distortion of the lattice at low temperatures. While the system undergoes a symmetry reduction from the cubic $Fm\bar{3}m$ space group at high temperature to the monoclinic $P21/n$ in the low-temperature regime, the magnetic atoms stay in an almost cubic unit cell, which leads to the uncommon helical structure. The experimental results of susceptibility and diffraction indicate that spin-orbit coupling in Ir^{+6} is negligible. The results strongly suggest that the system is not in a mixed $J_{eff} = 3/2$ and $J_{eff} = 1/2$ state due to band formation of the extended d orbitals as reported by Ou *et al.* The measured magnetic structure of Sr_2NiIrO_6 is intriguing and we are not aware of any other cubic or pseudocubic system that orders with an incommensurate propagation vector along the body diagonal. Apart from the incommensurate wave vector, the magnetic order of the iridium or nickel fcc sublattice is similar to the type-II order [19]. Both structures have ferromagnetically aligned moments on [111] planes. Since the J_1-J_2 magnetic phase diagram of the

fcc lattice does not contain incommensurate phases, further neighbor interactions have to be important in stabilizing the observed structure. Besides the strong further neighbor couplings that can be present in compounds with small charge gap, it is also possible to increase the relative weight of further neighbor interactions by the reduction of the first-neighbor exchange. This mechanism was proposed for the $5d^3$ double perovskites $La_2NaB'O_6$ ($B' =$ Ru, Os) [20,21] where only the B' site is magnetic. These compounds order with the $(0,0,k)$-type incommensurate propagation vector. The authors identify the large octahedral tilting being responsible for the reduction of first-neighbor $J_{B'\text{-}B'}$ couplings on the fcc lattice. However, the average octahedral tilting of 7° in Sr_2NiIrO_6 is much smaller than the value of 17° measured for $La_2NaB'O_6$. Thus, we expect the octahedral tilting to have a small effect in our system. To understand the origin of the magnetic order in Sr_2NiIrO_6 we have to consider both the exchange couplings within the fcc sublattices (iridium and nickel) and also the coupling between them.

The first-neighbor interactions between the iridium and nickel sublattices are expected to be ferromagnetic, where the main contribution to the exchange comes from the virtual electron hopping between the half-filled Ni e_g orbital and the empty Ir e_g orbitals. Further neighbor interactions between ions with identical valence state are expected to be antiferromagnetic. This intrinsic frustration must be important for stabilizing incommensurate magnetic order. Electronic structure calculations support the proposed opposite sign of the interactions with similar magnitude [11]. However, using the calculated exchange values up to second neighbor, mean-field theory would still give a commensurate type-III order [19]. Thus, more precise calculations and experimental studies such as resonant inelastic x-ray scattering [22] are necessary to unambiguously determine the spin Hamiltonian.

In conclusion, our study of Sr_2NiIrO_6 reveals a novel magnetic long-range order at low temperatures with an incommensurate propagation vector. The microscopic origin of the observed magnetic structure is the intrinsic frustration between the ferromagnetic coupling on nickel-iridium bonds and the antiferromagnetic coupling of the iridium-iridium bonds. The proposed mechanism provides a route to produce an incommensurate ground state in double perovskites with possible type-II multiferroicity induced by the spiral order.

The research leading to these results has received funding from the SNF project "Mott Physics Beyond the Heisenberg Model in Iridates and Related Materials." The work is based on neutron diffraction experiment performed at ISIS, UK and we thank Dr. A. Bhattacharyya for help on WISH. The magnetic susceptibility measurements were carried out on the MPMS device of the Laboratory for Scientific Developments and Novel Materials, Paul Scherrer Institute, Villigen, Switzerland.

[1] B. J. Kim, H. Ohsumi, T. Komesu, S. Sakai, T. Morita, H. Takagi, and T. Arima, Science **323**, 1329 (2009).
[2] Y. Singh and P. Gegenwart, Phys. Rev. B **82**, 064412 (2010).
[3] G. Jackeli and G. Khaliullin, Phys. Rev. Lett. **102**, 017205 (2009).
[4] F. Ye, S. Chi, H. Cao, B. C. Chakoumakos, J. A. Fernandez-Baca, R. Custelcean, T. F. Qi, O. B. Korneta, and G. Cao, Phys. Rev. B **85**, 180403 (2012).
[5] J. Reuther, R. Thomale, and S. Rachel, Phys. Rev. B **90**, 100405 (2014).
[6] K. Rolfs, S. Toth, E. Pomjakushina, D. Sheptyakov, J. Taylor, and K. Conder, Phys. Rev. B **91**, 180406(R) (2015).
[7] M. Ležaić and N. A. Spaldin, Phys. Rev. B **83**, 024410 (2011).
[8] M.-R. Li, M. Retuerto, Z. Deng, P. W. Stephens, M. Croft, Q. Huang, H. Wu, X. Deng, G. Kotliar, J. Sánchez-Benítez, J. Hadermann, D. Walker, and M. Greenblatt, Angew. Chem. **127**, 12237 (2015).
[9] A. A. Aczel, Z. Zhao, S. Calder, D. T. Adroja, P. J. Baker, and J.-Q. Yan, Phys. Rev. B **93**, 214407 (2016).
[10] P. Kayser, M. J. Martínez-Lope, J. A. Alonso, M. Retuerto, M. Croft, A. Ignatov, and M. T. Fernández-Díaz, Inorg. Chem. **52**, 11013 (2013).
[11] X. Ou, Z. Li, F. Fan, H. Wang, and H. Wu, Sci. Rep. **4**, 7542 (2014).
[12] J. Karpinski, Philos. Mag. **92**, 2662 (2012).
[13] G. Cao, J. Bolivar, S. McCall, J. E. Crow, and R. P. Guertin, Phys. Rev. B **57**, R11039 (1998).
[14] J. Zhao, L. Yang, Y. Yu, F. Li, R. Yu, and C. Jin, Inorg. Chem. **48**, 4290 (2009).
[15] Q. Zhao, F. Han, C. C. Stoumpos, T.-H. Han, H. Li, and J. F. Mitchell, Sci. Rep. **5**, 1 (2015).
[16] J. Rodríguez-Carvajal, Physica B **192**, 55 (1993).
[17] L. C. Chapon, P. Manuel, P. G. Radaelli, C. Benson, L. Perrott, S. Ansell, N. J. Rhodes, D. Raspino, D. Duxbury, E. Spill, and J. Norris, Neutron News **22**, 22 (2011).
[18] C. Holm and W. Janke, Phys. Rev. B **48**, 936 (1993).
[19] D. T. Haar and M. E. Lines, Philos. Trans. R. Soc. A **254**, 521 (1962).
[20] A. A. Aczel, D. E. Bugaris, L. Li, J.-Q. Yan, C. de la Cruz, H.-C. zur Loye, and S. E. Nagler, Phys. Rev. B **87**, 014435 (2013).
[21] A. A. Aczel, P. J. Baker, D. E. Bugaris, J. Yeon, H.-C. zur Loye, T. Guidi, and D. T. Adroja, Phys. Rev. Lett. **112**, 117603 (2014).
[22] W.-G. G. Yin, X. Liu, A. M. Tsvelik, M. P. M. Dean, M. H. Upton, J. Kim, D. Casa, A. Said, T. Gog, T. F. Qi, G. Cao, and J. P. Hill, Phys. Rev. Lett. **111**, 057202 (2013).